Eur. Phys. J. D **34**, 139–143 (2005)
DOI: 10.1140/epjd/e2005-00104-y

THE EUROPEAN PHYSICAL JOURNAL D

Rare earth based clusters for nanoscale light source

B. Masenelli[1,a], P. Mélinon[1], D. Nicolas[1], E. Bernstein[1], B. Prével[1], J. Kapsa[1], O. Boisron[1], A. Perez[1], G. Ledoux[2], B. Mercier[2], C. Dujardin[2], M. Pellarin[3], and M. Broyer[3]

[1] Laboratoire de Physique de la Matière Condensée et Nanostructures, Université Claude Bernard-Lyon1 et CNRS UMR 5586, Bâtiment Léon Brillouin, 6 rue Ampère, Domaine scientifique de la Doua, 69622 Villeurbanne Cedex, France
[2] Laboratoire de Physico-chimie des matériaux luminescents, Université Claude Bernard-Lyon1 et CNRS UMR 5620, Bâtiment Alfred Kastler, 10 rue Ampère, Domaine scientifique de la Doua, 69622 Villeurbanne Cedex, France
[3] Laboratoire de Spectrométrie Ionique et Moléculaire, Université Claude Bernard-Lyon1 et CNRS UMR 5620, Bâtiment Alfred Kastler, 10 rue Ampère, Domaine scientifique de la Doua, 69622 Villeurbanne Cedex, France

Received 6 September 2004
Published online 13 July 2005 –

Abstract. We investigate the fundamental properties of films resulting from the deposition of Eu^{3+} doped Gd_2O_3 clusters. We first report that the crystalline structure of clusters with diameter as low as 2.8 nm is still BCC (as in the bulk phase at ambient temperature and pressure). No phase transition to monoclinic structure is observed. We show that contamination from air (formation of hydroxide) is important and leads to the modification of the luminescence of the Eu^{3+} ions. Furthermore, films protected from this contamination have been fabricated and show a new feature (broad peak at 625 nm). It means that contamination is not the only mechanism responsible for the modification of the light emission spectrum. The crystal field symmetry breaking induced by the surface also plays a major role. Eventually, we show that the widening of the optical gap continues for these very small clusters. We discuss this effect in the frame of the quantum confinement model.

PACS. 36.40.Mr Spectroscopy and geometrical structure of clusters – 36.40.Vz Optical properties of clusters – 36.40.Jn Reactivity of clusters – 42.72.Bj Visible and ultraviolet sources – 61.46.+w Nanoscale materials: clusters, nanoparticles, nanotubes, and nanocrystals

1 Introduction

Nanophotonics is a rapidly growing field among nanoscience and nanotechnology topics. As so, it demands sources with nanometer dimensions capable of emitting light with a high efficiency, stable in time and under high excitation power. Several categories of materials are contemplated as potential candidates. Literature dealing with semiconductor nanoparticles, either of group IV (Si, Ge) [1–6] or II-VI (ZnS, CdSe...) [7–9], is abundant. These materials are primarily interesting because of their photo- and electroluminescence properties. Their light emission spectrum is usually centered in the visible range and broad (full width at half maximum of a few ten of nanometers). They also exhibit effects typical of their nanometer size. The first one is the dependence of the absorption gap and of the emission spectrum on the particle diameter. This effect is of quantum nature and is fairly described by the model of the delocalized Wannier-Mott exciton [10]. The confinement of a wide exciton within a small particle can lead to an increase in the optical gap as large as 0.6 eV for Si [11]. The second effect is the general fact that small particles have a large number of atoms on the surface compared to the number of bulk atoms. These surface atoms are usually responsible for non-radiative surface states or enhanced chemical reactivity which is often detrimental to the luminescence. That is the reason why Si or Ge nanoparticles need to be passivated (by oxygen in most of the cases or even hydrogen) in order to emit light. CdSe particles also need to have a protective shell to be stable [12–14]. Additionally, the luminescence of group IV semiconductors is typically rather small. II-VI semiconductor nanoparticles have higher quantum efficiency but are not stable under high excitation power. Their luminescence tends to be quenched with time. A second category of materials is the dye molecules family. These molecules exhibit very efficient luminescence in the visible range but are usually highly sensitive to high excitation power. Despite these drawbacks, the first nanophotonic systems based on these categories of materials become effective (in biological sensing for instance [15]). However, another category of promising materials exists. It is the class of rare-earth ions. Rare-earth ions are already widely used to produce light in many systems. For instance, Eu^{3+} and Tb^{3+} ions are used in cathode tube to produce red

[a] e-mail: Bruno.Masenelli@lpmcn.univ-lyon1.fr

and green light respectively. Er^{3+} ions are used for near-infrared telecommunications and several ions among the lanthanide family are used in solid state lasers. Their emission is rather bright, generally characterized by a high quantum efficiency, and stable in time even under high excitation power. Light-emitting rare-earth ions (Eu^{3+} and Tb^{3+}) can be incorporated in fluoride, bromide, chloride and oxide. We focus our attention on a referential oxide system (Gd_2O_3). This has two major advantages: to avoid luminescence quenching resulting from too high a concentration of luminescent ion (as it is the case in the pure oxides Eu_2O_3 and Tb_2O_3) on one hand and preserving the 3+ valence state of the ions necessary for luminescence on the other hand. It is therefore quite naturally that a still wider community has sought to synthesize nanoparticles from rare-earth oxides doped with light-emitting rare-earth ions. Three major effects due to the size reduction have been observed. The first one is a strong modification of the luminescence spectrum. As soon as the diameter of the particles is of the order of 6 nm or less, the sharp peaks of the spectrum, characteristic of the emission of an ion in a material of nearly perfect cristallinity, broaden and shift slightly. Several explanations have been evoked to account for this phenomenon. It has been proposed that the particles with very small dimensions distort their centered cubic crystal structure [16,17] and even turn to monoclinic structure, at least partially [18]. Also, since most of the particles from literature are produced by chemical routes, they always contain some residues of the solvent solution which perturb the luminescence spectrum [19]. It is therefore not straightforward to distinguish which mechanism is the most important one. The second size effect is the widening of the optical gap with the reduction of the particle size. Even though this effect is less pronounced than for semiconductors, it has been recently shown that the gap of Gd_2O_3 particles doped with Eu^{3+} ions increases from 5.4 eV to 5.55 eV as the particle diameter is reduced from 50 nm to 7 nm [20]. Surprisingly for iono-covalent materials such as these ones, this effect can be modeled by the quantum confinement model of the delocalized Wannier exciton. the third effect is a reduction of the decay time of luminescence. In this work, we have synthesized and analyzed films of Gd_2O_3 particles doped with Eu^{3+} ions (5% of the Gd ions substituted by Eu ions) by the Low Energy Cluster Beam Deposition technique (LECBD) with the smallest mean size reported yet (∼3 nm). First, it allows us to investigate on the possible structural transition from BCC to monoclinic for very small particles. In a second time, we evaluate the influence of surface contamination which is expected to be strongly enhanced at such small sizes. Eventually, we show that the gap widening continues even for particles with 3 nm diameter and that the quantum confinement model is still a valid description.

2 Experimental set-up

The cluster films have been deposited according to the LECBD technique described in details elsewhere [21]. Briefly, a target pellet made of a sintered powder of Gd_2O_3 doped with Eu^{3+} ions (5% of the Gd ions substituted by Eu ions) is hit by a pulsed (10 Hz repetition rate) YAG laser. The laser heating creates a plasma which is quenched by a synchronized helium burst (3 bars), starting the cluster nucleation. The plasma then undergoes a supersonic expansion through a nozzle. This adiabatic expansion freezes the nucleation of the clusters at an approximate rate of 10^{10} $K\,s^{-1}$. The cluster synthesis is far from the thermodynamic equilibrium conditions. The preformed clusters are then deposited on a substrate with sufficiently low kinetic energy (∼0.5 eV) to ensure they do not break upon deposition. Films for optical measurements have been deposited on LiF substrates whereas films for electronic structure analysis (XPS) have been deposited on deoxidized Si wafers. Two batches of samples have been fabricated: one at a pressure of 10^{-6} mbars and then put at air, the other one in ultra high vacuum (UHV) at a pressure of a few 10^{-9} mbars and then covered by a protective layer of LiF evaporated by Joule heating. During each deposition several samples have been deposited on carbon coated copper grids for high resolution transmission electron microscopy (HRTEM) measurements. The TEM analysis has been performed with a TOPCON microscope particularly adapted for high resolution measurement. The electronic states of the constituents have been investigated with a CLAM 4 VG X-ray photoelectron spectrometer with a mean resolution of 0.2 eV. We have used the Al-K line at 1486.6 eV and the calibration has been done with Au4f7/2 (84.0 eV), Ag3d5/2 (368.3 eV), Cu2p3/2 (932.6 eV) and Si2p (99.8 eV). The spectra have been corrected from background according to Shirley's procedure. The photoluminescence spectra have been recorded using a 450 W xenon lamp. An excitation wavelength of 307 nm was chosen from the spectrum of the lamp by a Jobin Yvon H10D monochromator. The emitted light was collected by an optical fiber and analyzed by a Triax 320 Jobin Yvon monochromator (resolution 0.05 nm) and a Peltier cooled charged coupled device detector. The absorption gap has been deduced from vacuum ultra violet (VUV) excitation spectra. The procedure is as follows. The light emitted between 605 nm and 625 nm is collected from the sample and measured as a function of the excitation wavelength. The VUV measurements have been carried out at 10K at the synchrotron radiation beamline SUPERLUMI of the DESY facility (Germany). The spectral resolution was 0.24 eV.

3 Results

3.1 Structural characterization

HRTEM has first provided us with the cluster size distribution. Two sets of samples have been synthesized with mean size of 2.8 nm and 3.2 nm by changing the volume of the nucleation chamber and the delay between the laser shot and the helium burst. HRTEM has also revealed the crystal structure of the clusters. Unambiguously, the BCC structure has been observed as can be seen in Figure 1. A representative cluster of 2.7 nm in diameter

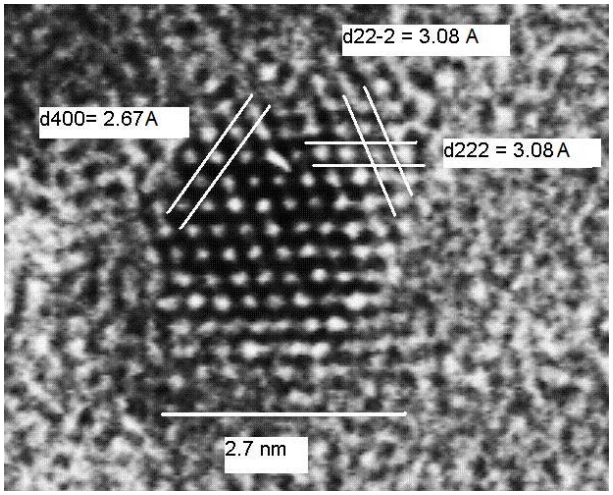

Fig. 1. HRTEM picture of a Eu^{3+} doped Gd_2O_3 cluster. The diameter of the cluster is 2.7 nm. Three distinct families of crystalline planes can be identified. The cluster points its $(1,\bar{1},0)$ direction towards the reader.

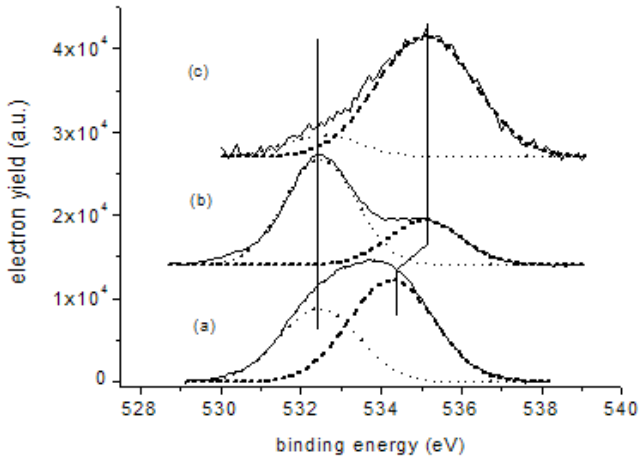

Fig. 2. Binding energy of the 1*s* electron of oxygen in (a) Eu^{3+} doped Gd_2O_3 clusters put at air, (b) Eu^{3+} doped Gd_2O_3 clusters annealed at 300 °C for 15 mn, (c) in $Gd(OH)_3$.

clearly shows three distinct families of planes. The BCC structure (Ia3 group 206) is the stable structure of Gd_2O_3 at ambient conditions of temperature and pressure. The measured crystal lattice is 10.65 Å which is equivalent to the nominal value of 10.81 Å within our accuracy. Because of our accuracy limit (0.2 Å) we cannot infer any contraction of the lattice parameter for small clusters. Only X-ray diffraction (XRD) measurements would confirm such a contraction. Unfortunately, our films are too thin to allow XRD measurements. Nevertheless, the key result is that despite the very small size of the clusters, the crystal structure does not change to the high temperature stable monoclinic structure (transition temperature of 1400 °C for bulk Gd_2O_3). Another striking observation (cf. Fig. 1) is that almost all diffracting particles are pointing their (110) direction towards the diffraction screen. It means that they are standing on a (110) face. Furthermore, one can see that the clusters have facets. If we consider that all these facets belong to the {110} family, the shape of the clusters is then, in the most symmetrical case, a rhombic dodecahedron. The rhombic dodecahedron is the shape of the first Brillouin zone of the Ia3 (group 206) structure. This structure is the densest that can be achieved considering the given ratio between the cation and anion radii. The observation of the densest possible structure for this compound means that the Coulomb interaction (ionic character) prevails over the covalent interaction here. This statement is not restricted to our synthesis method since the BCC structure is also observed for particles resulting from colloid synthesis [22].

3.2 Electronic characterization

In the case of a monoatomic rhombic dodecahedron structure, at sizes around 3 nm, roughly 40% of the atoms are standing on the surface. Even though we are not dealing with monoatomic clusters but with a diatomic compound, the fraction of surface atoms should not be very different from 40%. Since rare-earth oxides are usually sensitive to air moisture, we can expect a large contamination. Figure 2 shows the X-ray photoelectron spectroscopy (XPS) spectra of the O1*s* electron of O in our clusters that have been put at air, than annealed for 15 mn at 300 °C, along with the spectrum from $Gd(OH)_3$. One clearly sees two contributions in the O1*s* spectrum at 532.4 eV (dotted line) and 534.2 eV (dashed line), the latter being 1.5 times more intense than the former. When annealing the clusters at 300 °C for 15 mn, the intense peak shifts to the value of 535.5 eV which is the value of the O1*s* electron in gadolinium hydroxide. The ratio between the intensity of this peak and that of the peak at 532.4 eV is now reduced to 0.4. These two observations go to show that initially a major part of the oxygen is in the hydroxide form (dashed line). We have not reproduced hereafter the spectrum of the Gd3*d*5/2 electron since it does not present any change. The Gd3*d*5/2 electron spectrum is too large (at it is often the case for lanthanides) to be of any significant help.

3.3 Optical characterization

To further confirm the presence of a hydroxide shell around clusters that have been put at air, we have annealed the samples at temperatures ranging from 300 °C to 500 °C. Each temperature step has lasted 15 mn. Figure 3 shows the corresponding evolution of the main peak (around 610 nm) of the luminescence spectrum corresponding to the $4f^6\ {}^5D_0 \rightarrow 4f^6\ {}^7F_2$ transition. Two regimes can be distinguished. The first one occurs for an annealing temperature of 300 °C. A broad peak centered at 625 nm increases. This peak has not been reported in literature yet. Consistently with XPS analysis, we assign this peak to surface cleaning. An annealing at moderate temperature gets rid of hydroxide contamination on the surface. Consequently, the luminescence of most of the surface Eu^{3+} ions, previously quenched by the contamination

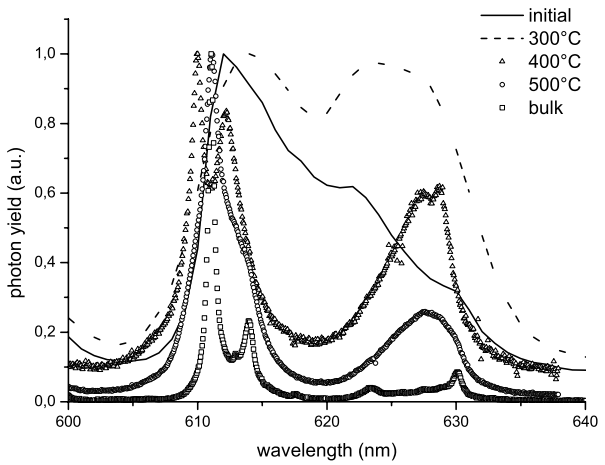

Fig. 3. Photoluminescence spectra of Eu^{3+} doped Gd_2O_3 clusters before and after a progressive annealing from 300 °C to 500 °C.

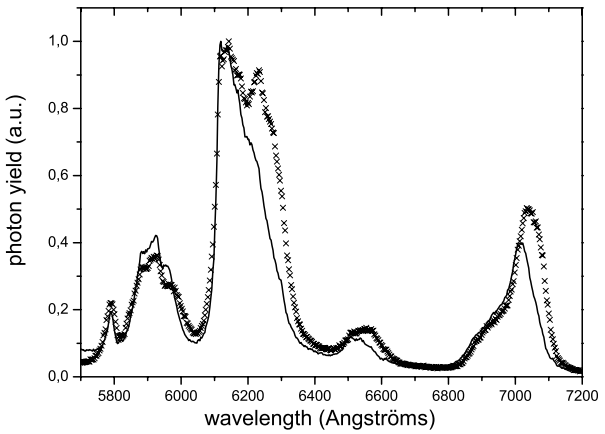

Fig. 4. Luminescence spectra of Eu^{3+} doped Gd_2O_3 clusters at air (solid line) and deposited in UHV and protected by a LiF capping layer (crosses).

shell, is now recovered. The total luminescence yield increases (area under the spectrum). In a second step, as the annealing temperature is increased, the peaks get sharper and tend to resemble to those of bulk Eu^{3+} doped Gd_2O_3. This is the result of cluster coalescence that leads to large particles where surface ions do not play a significant role anymore. A last confirmation of the presence of contamination is given by luminescence of the films deposited in UHV and protected by a LiF capping layer.

Figure 4 shows the corresponding spectrum along with that of the same unprotected film. The broad peak at 625 nm is present for the protected film. We can safely conclude that this peak results from Eu^{3+} ions on the surface of the clusters that are not contaminated. This emphasizes the need to have pure samples (not affected by any sort of contamination from air or any chemical solution) when discussing the effect of size reduction on the luminescence properties. It also suggests, since the spectrum of unpolluted clusters is not identical to that of bulk material, that the crystal field symmetry breaking induced

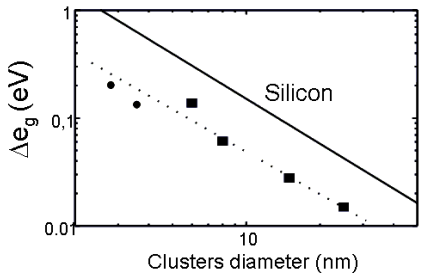

Fig. 5. Variation (in eV) of the optical gap of Eu^{3+} doped Gd_2O_3 clusters as a function of the cluster diameter. The circular marks correspond to the clusters studied in this work; the square marks are from reference [20]. The solid line is the result of quantum confinement model for silicon. The dotted line is the fit of experimental results on Gd_2O_3 clusters with the same quantum confinement model.

by the surface is a major mechanism in the modification of the luminescence properties. So far, we have been discussing the effect of size reduction on the luminescence of the doping ion. We now investigate the effect on the matrix optical gap. The main goal is to know whether the quantum confinement model is still valid for very small clusters. Optical gap values deduced from excitation measurements for two mean sizes have been plotted in Figure 5 along with previous results from Mercier et al. [20]. In the quantum confinement model, the gap variation E_g and the particle diameter d are linked by the following equation: $E_g = \alpha/d^{\gamma}$. (1) The striking result is that the simple quantum confinement model (dotted line) is still able to account for the gap variation of small clusters. In Figure 5 the slope of the fit line γ was equal to that of silicon, namely 1.39. We have already pointed out how surprising it is to see the validity of this model for ionocovalent materials. This simple model relies on the hypothesis of delocalized Wannier excitons which are not present in ionocovalent materials. Nevertheless, it looks as though a large part of the excitons in Gd_2O_3 are sensitive to the confinement. However, further investigation is needed to confirm the relevance of the model. Indeed, the α parameter is proportional to the Bohr radius of the exciton and depends also on the effective dielectric constant of the clusters. Taken into account the bulk value of ε for Gd_2O_3 (3.6 from Ref. [23]) and the theoretical value of the Bohr radius (0.5 nm) obtained by Bhargava et al. [24] with the LCAO method, it is not possible to fit our experimental data. Since little is known about these two quantities, we cannot draw a definite conclusion.

4 Conclusions

We have investigated the fundamental properties of films obtained from the deposition of Eu^{3+} doped Gd_2O_3 clusters. The first major result, concerning the crystalline structure, is that particles with diameters as low as 2.8 nm adopt the BCC structure (stable for the bulk phase at ambient temperature and pressure) rather than the monoclinic structure, stable at high temperature for the bulk

phase. The particles show facets and their shape is close to a rhombic decahedron. Secondly, the high ratio of surface atoms (∼40% of the total atoms) makes the clusters highly sensitive to contamination from air. The amount of contaminant species for samples put at air is high (more than 50% of the oxygen atoms). The contaminant species has been mainly identified as hydroxide. This contamination can be removed by an annealing at low temperature (300 °C for 15 mn) or avoided by protecting the samples with a capping LiF layer. The luminescence spectrum corresponding to unpolluted clusters is shown for the first time. An unreported broad peak at circa 625 nm is visible. The fact that the luminescence spectrum of pure clusters is still very different from that of bulk material suggests that the crystal field symmetry breaking induced by the surface is also a major mechanism controlling the light emission spectrum. Eventually, we have observed that the gap widening with the decrease of size already noticed for larger particles is still present for clusters with a mean size of 3.2 nm and 2.8 nm. Surprisingly, the quantum confinement model can describe this effect. However, a further effort has to be carried out to validate the use of this model for ionocovalent clusters.

This work has been done in the "Centre de Recherche Lyonnais sur les Agrégats". This work was supported by IHP-Contract No. HRPI-CT-1999-00040/2001-00140 of the European Commission. the authors are grateful to Marco Kirm and Irina Kamenskikh for their invaluable help on the SUPERLUMI line of DESY.

References

1. M. Zacharia, P.M. Fauchet, Appl. Phys. Lett. **71**, 380 (1997)
2. T. van Buuren, L.N. Dinh, L.L.Chase, W.J. Siekhans, L.J. Terminello, Phys. Rev. Lett. **80**, 3803 (1998)
3. C.E. Bottani, C. Mantini, P. Milani, M. Manfredini, A. Stella, P. Tognini, P. Cheyssac, R. Kofman, Appl. Phys. Lett. **69**, 2409 (1996)
4. A. Wellner, V. Paillard, C. Bonafos, H. Coffin, A. Claverie, B. Schmidt, H. Heinig, J. Appl. Phys. **94**, 5639 (2003)
5. S. Sato, S. Nozaki, H. Morisaki, M. Iwase, Appl. Phys. Lett. **66**, 3176 (1995)
6. G. Ledoux, O. Guillois, D. Porterat, C. Reynaud, F. Huisken, B. Kohn, V. Paillard, Phys. Rev. B **62**, 15942 (2000)
7. C.B. Murray, D.J. Norris, M.G. Bawendi, J. Am. Chem. Soc. **115**, 8706 (1003)
8. V. Colvin, M. Schlaub, A.P. Alivisatos, Nature **370**, 314 (2000)
9. V.I. Klimov, A.A. Mikhailovsky, S. Xu, J.A. Hollingsworth, C.A. Leatherdale, H.-J. Eisler, M.G. Bawendi, Science **290**, 314 (2000)
10. L.E. Brus, J. Phys. Chem. **90**, 2555 (1986)
11. G. Ledoux, J. Gong, F. Huisken, O. Guillois, C. Reynaud, Appl. Phys. Lett. **80**, 4834 (2002)
12. M. Bruchez, M. Moronne, P. Gin, S. Weiss, A.P. Alivisatos, Science **281**, 2013 (1998)
13. M.A. Hines, P. Guyot-Sionnest, J. Phys. Chem. **100**, 468 (1996)
14. N. Myung, Y. Bae, A.J. Bard, Nano Lett. **3**, 747 (2003)
15. W.C. Chan, S. Nie, Science **281**, 2016 (1998)
16. W.W. Zhang, W.-P. Zhang, P.-B. Xie, M. Yin, H.-T. Chen, L. Jing, L.-R. Lou, S.-D. Xia, J. Coll. Inter. Sci. **262**, 588 (2003)
17. T. Igarashi, M. Ihara, T. Kusunoki, K. Ohno, T. Isobe, M. Senna, Appl. Phys. Lett. **76**, 1549 (2000)
18. D.K. Williams, H. Yuan, B.M. Tissue, J. Lumin. **83-84**, 297 (1999)
19. P.K. Sharma, R. Nass, H. Schmidt, Opt. Mat. **10**, 161 (1998)
20. B. Mercier, C. Dujardin, G. Ledoux, C. Louis, O. Tillement, P. Perriat, J. Appl. Phys. **96**, 651 (2004)
21. M. Pellarin, C. Ray, J. Lermé, J.L. Vialle, M. Broyer, P. Mélinon, J. Chem. Phys. **112**, 8436 (2000)
22. C. Louis, R. Bazzi, M.A. Flores, W. Zheng, K. Lebou, O. Tillement, B. Mercier, C. Dujardin, P. Perriat, J. Sol. State Chem. **173**, 335 (2003)
23. A. Garcia-Murillo, C. Leluyer, C. Garapon, C. Dujardin, E. Bernstein, C. Pedrini, J. Mugnier, Opt. Mater. **19**, 161 (2002)
24. R.N. Barghava, J. Cryst. Growth **214-215**, 926 (2000)